Available online at www.sciencedirect.com
SCIENCE DIRECT®
Journal of Electroanalytical Chemistry 587 (2006) 31–41
Journal of Electroanalytical Chemistry
www.elsevier.com/locate/jelechem

The reduction of L-cystine in hydrochloric acid at mercury drop electrodes

T.R. Ralph [a,b,d], M.L. Hitchman [a], J.P. Millington [c], F.C. Walsh [d,*]

[a] Department of Pure and Applied Chemistry, University of Strathclyde, 295 Cathedral Street, Glasgow G1 1XL, UK
[b] Johnson Matthey Fuel Cells, Lydiard Fields, Great Western Way, Swindon SN5 8AT, UK
[c] School of Chemical Engineering and Analytical Science, University of Manchester, Sackville Street, Manchester M60 1QD, UK
[d] Electrochemical Engineering Group, School of Engineering Sciences, University of Southampton, Room 1001, Building 30, Highfield, Southampton SO17 1BJ, UK

Received 3 March 2005; received in revised form 11 August 2005; accepted 6 October 2005
Available online 15 December 2005

Abstract

The reduction of L-cystine in 0.1 mol dm^{-3} HCl at 298 K has been studied at mercury electrodes. Dropping mercury electrode (DME), static mercury drop electrode (SMDE) and hanging mercury drop electrode (HMDE) modes were used with normal, sampled d.c. and differential pulse polarographic detection. The charge transfer kinetics for the irreversible reduction of L-cystine were complicated by reactant and product adsorption, by the formation of cysteinate complexes between mercury and the product thiol as well as by formation of Hg_2Cl_2. High Tafel slopes of −182 mV per decade were observed with a cathodic transfer coefficient of 0.32. The diffusion coefficient of L-cystine was found to be 5.3×10^{-10} m^2 s^{-1} in 0.1 mol dm^{-3} HCl and 4.2×10^{-10} m^2 s^{-1} in 2.0 mol dm^{-3} HCl at 298 K. The mechanism of L-cystine reduction at mercury has been discussed and the effects of pH and reactant concentration have been quantified.

Keywords: Amino acids; Disulphide adsorption; Cysteinate formation; L-cystine; L-cysteine; Mercury electrodes; Linear sweep voltammetry; Cyclic voltammetry; Polarography; HMDE; SMDE; DME

1. Introduction

The literature on the reduction of L-cystine to L-cysteine has been reviewed from the perspectives of electrosynthesis [1] and electrode kinetics [2]. Previous studies have considered the effect of electrode materials, cell design and process conditions on the efficiency of the reduction [3–8]. The reactant disulphide and the product thiol have a low solubility at pH > 2 but both are soluble at concentrations up to approximately 1 mol dm^{-3} in 2 mol dm^{-3} HCl. In hydrochloric acid media, the reduction of the disulphide can be represented by

$$RSSR + 2H^+ + 2e^- \rightarrow 2RSH \quad (1)$$

where $R = CH_2(NH_3.HCl)COOH$. In a series of papers, the electrosynthesis of L-cysteine at solid cathodes has been described with regard to mathematical models based on fractional conversion and the reactor performance has been discussed in terms of classical figures of merit [6–8]. A wide range of electrode materials has been evaluated [6–9] including mercury and lead [7]. Despite the toxicity of these metals, it is possible to control the operational conditions such that the L-cysteine produced has an acceptably low metal ion content.

In acid electrolytes, the evolution of hydrogen

$$2H^+ + 2e^- \rightarrow H_2 \quad (2)$$

is very competitive with reaction (1). In order to achieve a high current efficiency for electrosynthesis of the thiol and quantitative kinetic data for reduction of the disulphide, it is important to use a high hydrogen overpotential cathode. A previous paper has described the use of lead rotat-

* Corresponding author. Tel.: +44 2380 598752; fax: +44 2380 598754.
E-mail address: F.C.Walsh@soton.ac.uk (F.C. Walsh).

0022-0728/$ - see front matter © 2005 Elsevier B.V. All rights reserved.
doi:10.1016/j.jelechem.2005.10.005

Nomenclature

A	electrode area, m^2
b_c	cathodic Tafel slope, V $decade^{-1}$
c_b	bulk reactant concentration, mol m^{-3}
D	diffusion coefficient of reactant, $m^2\ s^{-1}$
E	electrode potential, V
$E_{1/2}$	half wave potential, V
$E^{o\prime}$	standard formal potential, V
F	Faraday constant, 96,485 C mol^{-1}
$F_2\ (\chi)$	function defined by Eq. (12)
I	current, A
j	current density, A m^{-2}
j_L	limiting current density, A m^{-2}
k^o	heterogeneous rate constant at $E^{o\prime}$, m s^{-1}
k_f^o	heterogeneous rate constant (at 0 V vs. SCE), m s^{-1}
k_f	heterogeneous rate constant for forward (cathodic) process, m s^{-1}
m	electrochemical reaction order
$\frac{dw}{dt}$	mass flow rate of mercury, mg s^{-1}
q_p	electrical charge under voltammogram peak, C
r	radius of mercury drop, m
R	molar gas constant, 8.314 J K^{-1} mol^{-1}
t	time, s
v	potential sweep rate, V s^{-1}
z	number of electrons in the electrode process
Greek	
α_c	cathodic transfer coefficient
β'	adsorption coefficient
λ	function defined by Eq. (8)
τ	surface excess of adsorbate
τ_s	saturation coverage value of τ
$\chi(bt)$	function defined by Eq. (16)
$\Phi(bt)$	function defined by Eq. (17)
θ	surface coverage

ing disc electrodes to extract kinetic parameters and the diffusion coefficient of L-cystine [10]. For kinetic studies, mercury cathodes offer the advantage of a liquid metal having a readily renewable surface together with a high hydrogen overpotential. While there are published papers on the polarography of the L-cysteine/L-cystine redox couple [1], studies in hydrochloric acid are very limited. In particular, previous work has been restricted to low concentrations of the amino acids which are of little interest to electrosynthesis of the thiol. The charge transfer kinetics in hydrochloric acid are complicated by the formation of calomel (Hg_2Cl_2) in addition to adsorption of the disulphide and to mercury cysteinate complex formation with the product thiol.

In this paper, the disulphide reduction is studied in aqueous 0.1 and 2.0 mol dm^{-3} HCl at a dropping mercury electrode (DME), a static mercury drop electrode (SMDE) and a hanging mercury drop electrode (HMDE). This range of mercury drop geometries, together with careful attention to electrolyte composition, polarographic mode and experimental procedure, allows quantitative charge transfer data to be obtained.

2. Experimental details

An EG&G PARC Model 303A static mercury drop electrode system was employed. Polarographic grade, triply distilled mercury (Belgrave Mercury Ltd.) was employed. The cell, a glass cup of volume 20 cm^3, was located beneath an electrode support block, which contained the mercury capillary working electrode, a platinum wire counter electrode, an Ag|AgCl reference electrode, a drop dislodge mechanism, a plastic sparge tube to purge the electrolyte with nitrogen and a port through which the cell was automatically blanketed with nitrogen during measurements. The electrode could be operated in the DME, SMDE or HMDE mode.

The mercury drop electrode assembly was fitted with a Model G0199 glass capillary. The capillary bore was siliconised with EG&G PARC G0092 solution to minimise penetration by the electrolyte. Two capillaries were used which gave mercury drops of geometrical area 0.021 and 0.014 cm^2, these values being determined by weighing a measured number of drops. The 3.8 mol dm^{-3} KCl, saturated with AgCl internal electrolyte, was changed weekly to preclude potential drift.

The majority of studies involved HCl based electrolytes. BDH Analar grade L-cystine and L-cysteine were used as supplied, typically in aqueous 0.1 or 2.0 mol dm^{-3} HCl at 298 K. The effect of pH on the system was investigated using aqueous chloride solutions of constant ionic strength (0.5 mol dm^{-3}) and pH. Solution compositions were obtained from a collection of data on buffer solutions [11]. For pH 1.1 to pH 2.0, HCl/KCl solutions were used, pH 2.2 to pH 8.0 involved $Na_2HPO_4 \cdot 12H_2O$/$C_6H_8O_7 \cdot H_2O$/KCl, pH 8.0 to 10.0 utilised H_3BO_3/KOH and pH 12.0 and pH 13.0 used NaOH/KCl.

Voltammograms were recorded using an EG&G PARC Model 174A polarographic analyser while potential sweep rates were controlled using a Thompson DRG16 sweep generator. The current output was monitored with a Houston 2000 XY chart recorder. The polarographic equipment was validated using an aqueous mixture of copper (II), lead (II) and cadmium (II) ions in aqueous 0.1 mol dm^{-3} nitric acid at 298 K. $E_{1/2}$ values from sampled d.c. polarograms of −0.08, −0.40 and −0.60 V vs. SCE, respectively, agreed with the published literature [12].

Steady state voltammograms were recorded by sweeping the electrode potential from the initial to the final potential limit then back to the initial potential (to check for hysteresis) at a rate of 2 mV s^{-1}. Linear sweep and cyclic voltammograms were recorded by sweeping the mercury electrode potential between the potential limits at sweep rates of between 25 and 500 mV s^{-1}. The electrolytes were deoxygenated with nitrogen for an hour prior to measurements and the cell was blanketed with nitrogen during measurements to prevent air ingress.

Solution viscosity was determined by standard u-tubes in a Gallenkamp viscometer bath and solution density was determined using density bottles. A Corning 150 pH/Ion Meter and Ingold pH electrode were used to measure solution pH.

3. Results and discussion

3.1. L-cystine reduction in hydrochloric acid electrolyte

3.1.1. Cyclic voltammetry at a HMDE

Cyclic voltammograms of 0.1 mol m^{-3} L-cystine in aqueous 0.1 mol dm^{-3} HCl at the HMDE are in accord with the literature for other electrolytes [13]. Fig. 1 shows the response at a potential sweep rate of 100 mV s^{-1}. The peak at −0.125 V vs. SCE is due to the reduction of adsorbed L-cystine to L-cysteine

$$RSSR_{(ads)} + 2H^+ + 2e^- \rightarrow 2RSH \quad (3)$$

The reduction rate is controlled by the rate of adsorption of the reactant at the mercury surface, as shown by a linear dependence of j_p on v. The major peak at −0.450 V vs. SCE corresponds to the irreversible, diffusion controlled reduction of L-cystine, according to reaction (1). As expected, j_p is proportional to $v^{1/2}$ and to the reactant concentration.

The L-cysteine produced in the negative potential scan is reversibly oxidised to mercury cysteinate

$$2RSH + 2Hg - 2e^- \rightleftharpoons (RS)_2Hg_{2(ads)} + 2H^+ \quad (4)$$

$$2RSH + Hg - 2e^- \rightleftharpoons (RS)_2Hg_{(ads)} + 2H^+ \quad (5)$$

The oxidation is diffusion controlled and j_p is directly proportional to $v^{\frac{1}{2}}$ and to the L-cysteine concentration. During the second potential scan, mercury (I) cysteinate is reduced to L-cysteine, according to reactions (4) and (5), at a peak potential of −0.130 V vs. SCE. Fig. 1 shows that the peak completely swamps the current for reduction of adsorbed L-cystine, according to reaction (3). At L-cysteine concentrations less than or equal to 0.1 mol m^{-3}, the rate of reduction of the mercury cysteinate (produced by the oxidation of the thiol) is directly proportional to the potential sweep rate, confirming that the rate of reduction is controlled by adsorption of mercury cysteinate at the electrode surface.

At disulphide and thiol concentrations higher than 0.1 mol m^{-3}, two cathodic and two anodic peaks are evident for electrode reactions (4) and (5), as shown in

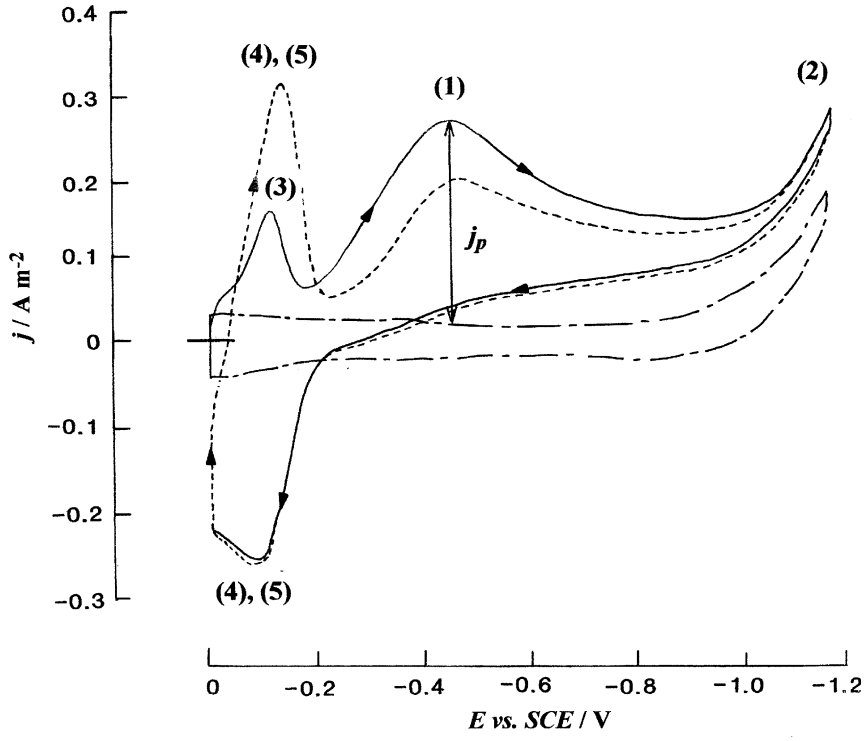

Fig. 1. Cyclic voltammetry of 0.1 mmol dm^{-3} L-cystine in aqueous 0.1 mol dm^{-3} HCl at a HMDE at a potential sweep rate of 100 mV s^{-1}. The electrolyte was deoxygenated with N_2 at 298 K. The peaks are labelled with reaction numbers from the text: (1) reduction of L-cystine, (3) reduction of adsorbed L-cystine, (4,5) oxidation of L-cysteine to mercury cysteinates. (——) first sweep; (· · · · · ·) second sweep; (-·-·-·-·-) background electrolyte.

Fig. 2. This is attributable to the rearrangement of mercury cysteinate on the electrode surface. Stankovich and Bard [13] have alluded to this effect although, at pH 7.4, they observed sharp spikes on the original peaks rather than an additional peak.

Significantly, hydrogen evolution at mercury surfaces does not commence in aqueous 0.1 mol dm^{-3} HCl until a potential as negative as −0.9 V vs. SCE (Fig. 1). This allows the reduction of L-cystine to be clearly defined at less negative potentials in the voltammetry.

3.2. Differential pulse and sampled d.c. polarograms at a DME

The sampled d.c. and differential pulse polarograms of 0.1 mol m^{-3} L-cystine in aqueous 0.1 mol dm^{-3} HCl are shown in Figs. 3(a) and (b), respectively. As expected from the cyclic voltammetry, differential pulse voltammograms show two peaks for reduction of adsorbed (E_p at −0.125 V vs. SCE) and dissolved (E_p at −0.450 V vs. SCE) L-cystine to L-cysteine, according to reactions (3) and (1), respectively. Sampled d.c. polarograms consist of a single irreversible wave with $E_{1/4}$, $E_{1/2}$ and $E_{3/4}$ values of −0.29, −0.35 and −0.43 V vs. SCE. According to the Tomes criterion, the wave is very irreversible with $|E_{3/4} - E_{1/4}| = 140\ \text{mV} > > 56.4/z$ mV at 298 K. The complexity of the electrode process is not readily observed using d.c. polarography. The irreversible wave does show a well defined diffusion limited current above −0.5 V (vs. SCE). Below −0.5 V vs. SCE, the reduction of dissolved L-cystine is under mixed (kinetic-mass transport) control followed by pure kinetic control at potentials close to the open-circuit value.

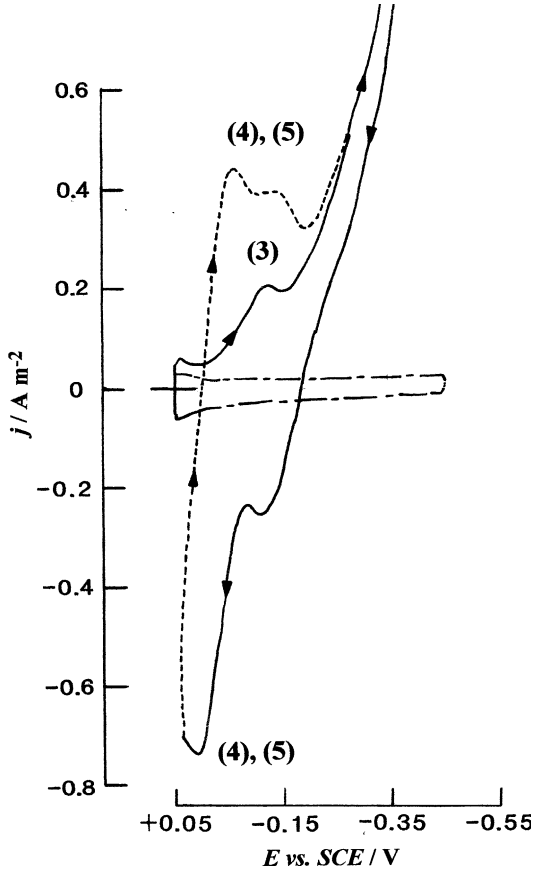

Fig. 2. Cyclic voltammetry of 0.25 mmol dm^{-3} L-cystine in aqueous 0.1 mol dm^{-3} HCl at a HMDE. Potential sweep rate 100 mV s^{-1}. The electrolyte was deoxygenated with N_2 at 298 K. (——) first sweep; (·····) second sweep; (----------) background electrolyte. The numbers in parenthesis refer to reaction numbers in the text.

3.3. Electrochemistry under typical electrosynthesis conditions

Much higher disulphide concentrations (0.01–0.7 mol dm^{-3}) and thiol concentrations (0–1.4 mol dm^{-3}) in aqueous 2.0 mol dm^{-3} hydrochloric acid are typically present during the electrosynthesis of L-cysteine. At L-cystine concentrations higher than 0.1 mmol dm^{-3}, there are no published reports on the voltammetry at mercury in acid electrolytes. Fig. 4(a) shows the cyclic voltammetry of 0.75 mmol dm^{-3} L-cystine in aqueous 0.1 M mol dm^{-3} HCl at a HMDE. There is a complete blockage of the electrode surface by the amino acids on the cathodic scan and a sharp change in the current in the return anodic scan which is due to the removal of the surface blocking. Even when the mercury drop is replenished during sampled d.c. polarograms (Fig. 4(b)) a large capillary maximum is produced and differential pulse polarograms (Fig. 4(c)) show sharp changes in the current. The voltammograms provide direct evidence for the strong adsorption of both the disulphide and the thiol at the mercury electrode.

Cyclic voltammograms in aqueous 2.0 mol dm^{-3} hydrochloric acid show the reported [14] reversible peaks for calomel formation in the potential range of +0.2 to −0.2 V vs. SCE

$$Hg_2Cl_2 + 2e^- \rightleftharpoons 2Hg + 2Cl^- \qquad (6)$$

This reaction masks the peak due to the reduction of adsorbed L-cystine and the peaks due to the irreversible oxidation of the thiol to mercury cysteinates. In cyclic voltammograms and sampled d.c. and differential pulse polarograms, the irreversible, diffusion controlled reduction of solution phase L-cystine to L-cysteine is still evident. In cyclic voltammograms, it is possible to study the electrosynthesis reaction free of the electrochemistry of calomel by using a positive potential limit of −0.2 V vs. SCE.

3.4. Kinetic parameters

The cyclic voltammograms and sampled d.c. polarograms can be analysed to determine the kinetic parameters for the reduction of dissolved L-cystine to L-cysteine according to reaction (1).

For sampled d.c. polarograms, the equation

$$-\log\left[\frac{1}{j} - \frac{1}{j_L}\right] = -\frac{\alpha_c F}{2.303RT}E + \log(zFk_f^o\ c_b) \qquad (7)$$

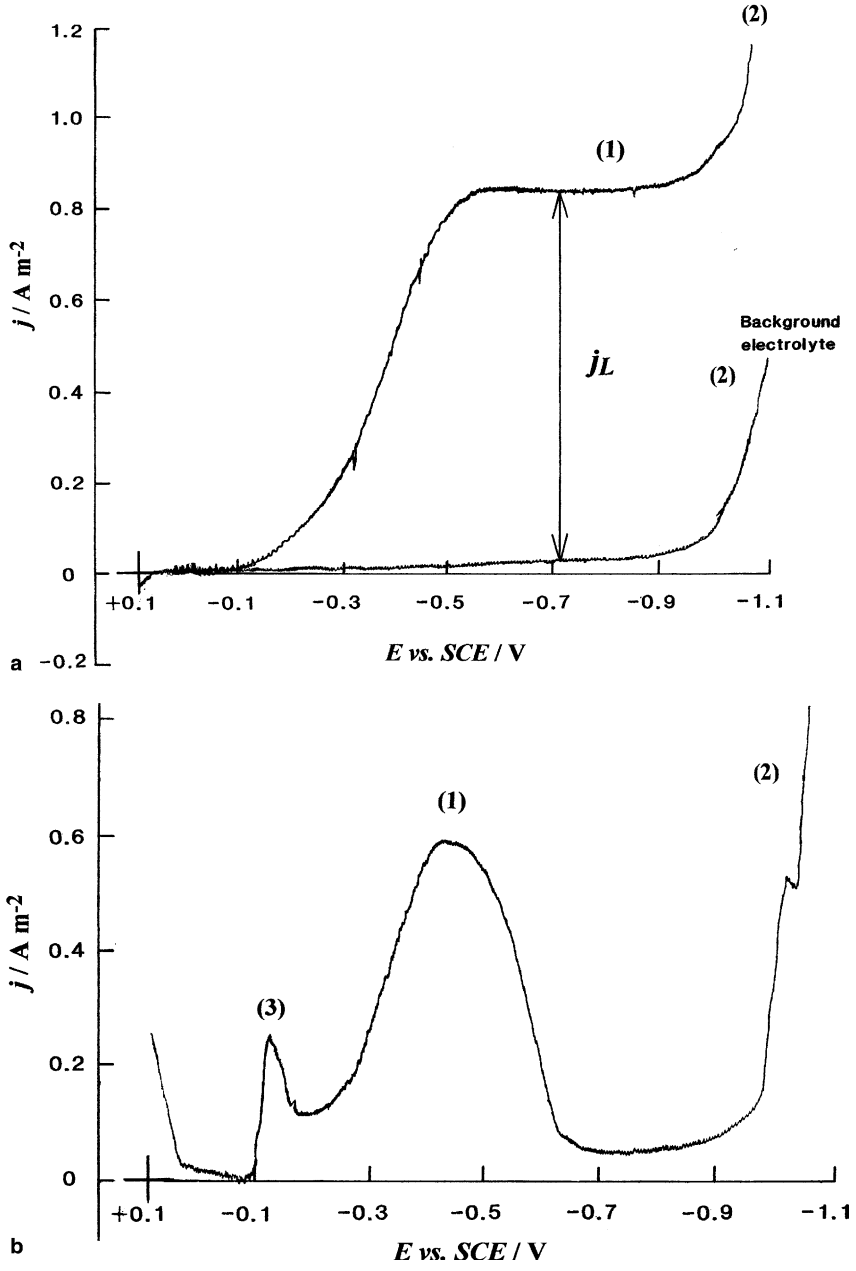

Fig. 3. Linear sweep voltammograms at a SMDE. (a) sampled d.c. and (b) differential pulse (amplitude modulation = 25) modes for reduction of 0.1 mmol dm^{-3} L-cystine in 0.1 mol dm^{-3} HCl deoxygenated with N_2 at 298 K. 1 drop s^{-1}. $v = 2$ mV s^{-1}. The numbers in parenthesis refer to reaction numbers in the text.

may be applied [15], where j is the current density, j_L the limiting current density, α_c is the cathodic transfer coefficient, E is the electrode potential, k_f^o is the standard heterogeneous rate constant and c_b is the bulk reactant concentration.

Fig. 5 shows the mass transfer corrected Tafel plot for the polarogram in Fig. 3, from which the diffusion limited current density was readily calculated. A small background current, shown in Fig. 3, was subtracted at the limiting current. From the Tafel plot, at 298 K, the Tafel slope is -183 ± 2 mV $decade^{-1}$ and α_c is 0.32 ± 0.01.

There is an alternative method of obtaining the kinetic parameters from the sampled d.c. polarograms although this has the disadvantage of requiring accurate values of the reactant diffusion coefficient. For an electrochemically, irreversible first-order reaction, under mixed kinetic-mass transport control the time-dependent current density (assuming semi-infinite linear diffusion) is given by [16]

$$j = \left(\frac{zFD^{1/2}c_b}{t^{1/2}}\right)\lambda \exp(\lambda^2)\mathrm{erfc}(\lambda), \tag{8}$$

where

$$\lambda = k_f t^{1/2}/D^{1/2}. \tag{9}$$

Here, k_f is the heterogeneous rate constant and D is the diffusion coefficient of L-cystine.

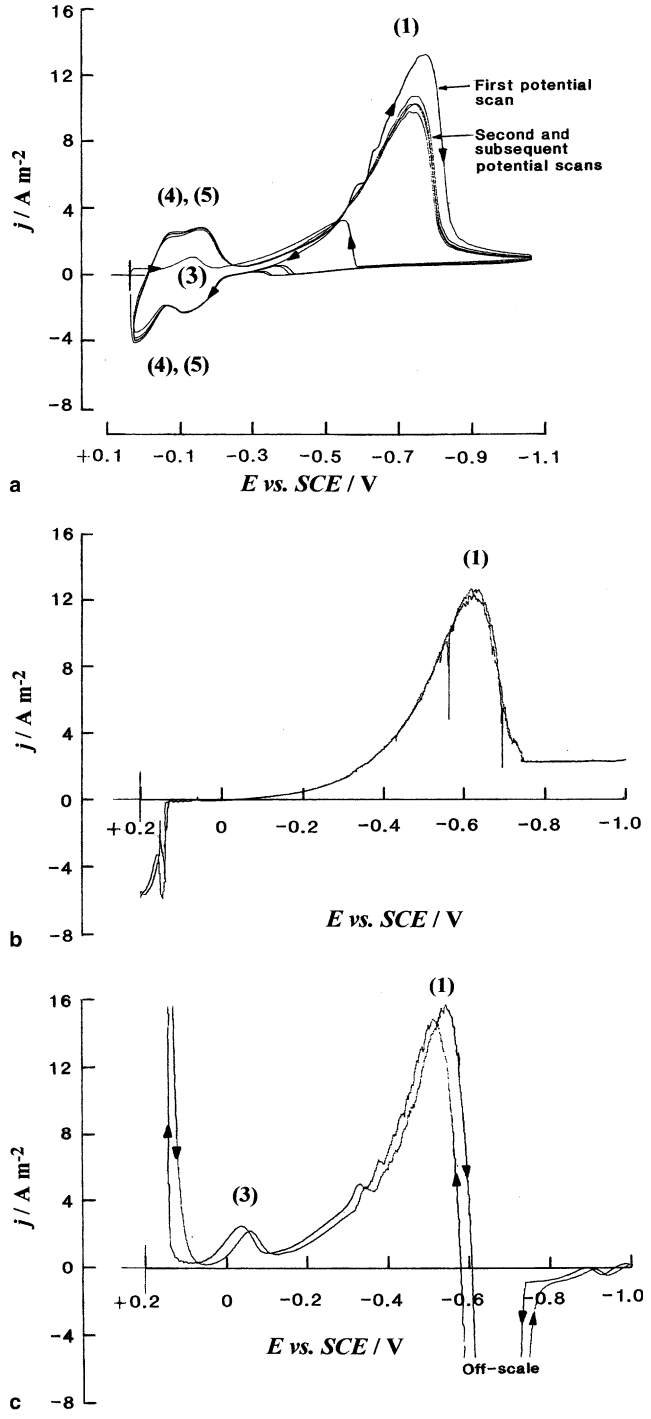

Fig. 4. Voltammograms for reduction of 0.75 mmol dm^{-3} L-cystine in 0.1 mol dm^{-3} HCl. The electrolyte was deoxygenated with N_2 at 298 K. (a) cyclic voltamogram at a HMDE, $v = 100$ mV s^{-1}, (b) sampled d.c. polarogram at an SMDE, 1 drop s^{-1}, $v = 2$ mV s^{-1} and (c) differential pulse polarogram at an SMDE, 1 drop s^{-1}, $v = 2$ mV s^{-1}, (amplitude modulation = 25). Numbers in parenthesis refer to reactions in the text.

The diffusion limited current density is given by the Cottrell equation

$$j_L = \frac{zFD^{1/2}c_b}{(\pi t)^{1/2}}. \tag{10}$$

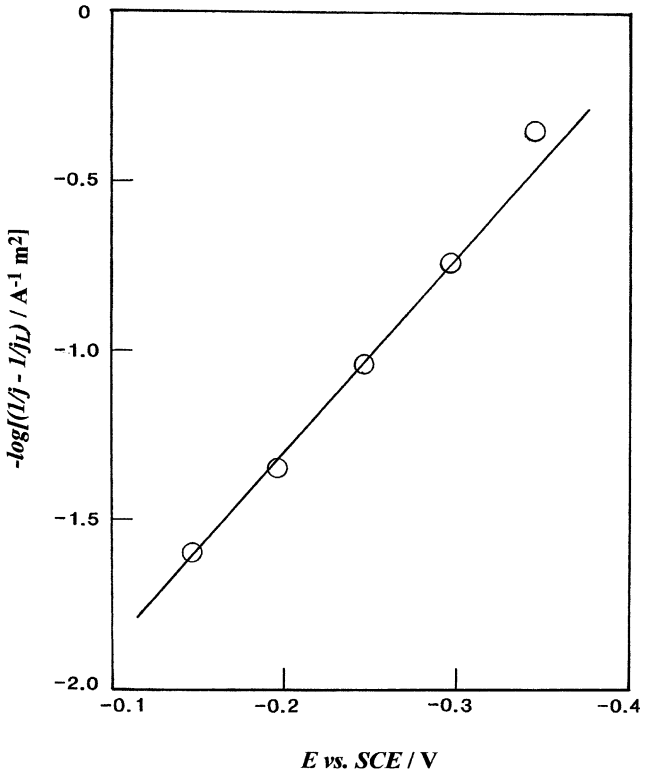

Fig. 5. Mass transport corrected Tafel plot for reduction of L-cystine at a SMDE. 0.1 mmol dm^{-3} L-cystine in 0.1 mol dm^{-3} HC deoxygenated with N_2 at 298 K. The background current has been subtracted.

Combining Eqs. (8) and (10) gives

$$\frac{j}{j_L} = \pi^{1/2}\lambda \exp(\lambda^2)\mathrm{erfc}(\lambda). \tag{11}$$

This equation must be modified for a DME due to the stretching effect. At any selected time, expansion of the drop causes the thickness of the diffusion layer to be reduced so that larger currents flow essentially increasing the diffusion coefficient. Koutecky solved this problem rigorously and expressed the result in terms of a ratio of the current density to the limiting current density via a power series function [17,18]

$$\frac{j}{j_L} = F_2(\chi), \tag{12}$$

where $F_2(\chi)$ is a numerical function computed from a power series [17,18].

From a sampled d.c. polarogram measurement of j/j_L yields $F_2(\chi)$ and since $\chi = (12/7)^{1/2}k_f t^{1/2}/D^{1/2}$ if the diffusion coefficient of the reactant is known k_f is obtained. A plot of $\log k_f$ against E, according to

$$\log k_f = \log k_f^o + b_c \cdot E \tag{13}$$

provides the kinetic parameters, where the cathodic Tafel slope is

$$b_c = -\frac{2.303RT}{\alpha_c zF}. \tag{14}$$

Table 1 lists values of j/j_L measured from the polarogram in Fig. 3, the corresponding $F_2(\chi)$ value and the calculated

k_f values at the cathode potential corresponding to the current density, j, assuming the diffusion coefficient of L-cystine is 5.0×10^{-10} m^2 s^{-1} at 298 K.

The plot of log k_f against E is shown in Fig. 6; as predicted by Eq. (13) a straight line relationship is obtained. From the gradient, using a linear least squares regression analysis, the Tafel slope is -183 ± 4 mV decade^{-1} and α_c is 0.32 ± 0.02. Within the limit of experimental error, these values are identical to those obtained from the mass transport corrected Tafel plot. This provides strong support for the validity of the diffusion coefficient used in the kinetic analysis.

It is also possible to obtain the kinetic parameters from an analysis of the main peak for reaction (3) in the cyclic voltammograms. Nicholson and Shain [19] have shown that the current density at an HMDE may be expressed in terms of planar and spherical contributions

$$j = j_{(\text{planar})} + j_{(\text{spherical})}, \tag{15}$$

where the planar and spherical diffusion limited current densities are given by

$$j_{(\text{planar})} = zFc_b D^{1/2} v^{1/2} \left[\frac{\alpha_c F}{RT}\right] \pi^{1/2} \chi(bt), \tag{16}$$

$$j_{(\text{spherical})} = zFc_b D \left[\frac{1}{r}\right] \Phi(bt). \tag{17}$$

Here, r is the drop radius while $\chi(bt)$ and $\Phi(bt)$ are current functions.

At potential sweep rates above 100 mV s^{-1}, spherical diffusion has little effect upon E_p as shown by the lack of change in the peak current; at lower potential sweep rates, however, $I_{(\text{total})}$ and E_p move in the cathodic direction. Using these higher sweep rates, for L-cystine reduction at a HMDE, Eq. (16) should still apply with $\pi^{1/2}\chi(bt) = 0.4958$. Under such conditions

$$E_p = E^{o'} - \frac{RT}{\alpha_c F}\left[0.780 + 2.303 \log\left(\frac{D^{1/2}}{k^o}\right) + 2.303 \log\left(\frac{\alpha_c F v}{RT}\right)^{1/2}\right], \tag{18}$$

where $E^{o'}$ is the standard formal potential. k^o can be converted to k_f^o by assuming a value for $E^{o'}$. As noted elsewhere [1,2], it is difficult to establish a meaningful standard formal potential for the cysteine/cystine redox couple due to its irreversibility.

Table 1
Values of heterogeneous rate constant, k_f, from sampled d.c. polarography

E/V vs. SCE	j/j_L	$F_2(\chi)$	k_f/m s^{-1}
−0.395	0.740	2.5	4.3×10^{-5}
−0.345	0.530	1.146	2.0×10^{-5}
−0.295	0.341	0.555	9.5×10^{-6}
−0.245	0.213	0.292	5.0×10^{-6}
−0.195	0.130	0.168	2.9×10^{-6}
−0.145	0.073	0.088	1.5×10^{-6}

0.1 mmol dm^{-3} L-cystine in 0.1 mol dm^{-3} HCl at 298 K. $D = 5.0 \times 10^{-10}$ m^2 s^{-1}. 1 drop s^{-1}.

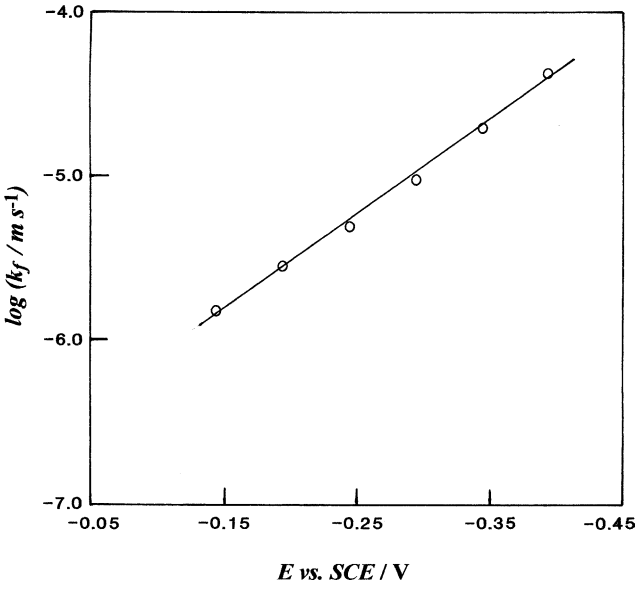

Fig. 6. Semilogarithmic plot of the heterogeneous rate constant for reduction of L-cysteine vs. the electrode potential.

A plot of E_p against log v should be a straight line giving b_c and α_c from the gradient. At lower sweep rates, deviation from linearity is expected. Fig. 7 shows a typical plot of E_p against log v for L-cystine reduction at the HMDE. The negative shift in E_p at potential sweep rates at and below 100 mV s^{-1} is evident. From a least squares analysis of the remaining points, b_c is -187 ± 6 mV decade^{-1} and α_c is 0.32 ± 0.02 (assuming D is 5.0×10^{-10} m^2 s^{-1} at 298 K).

Table 2 compares the kinetic parameters obtained from the sampled d.c. polarography and from linear sweep voltammetry. The close comparison between the values obtained provides strong evidence for the accuracy of the kinetic parameters. For 0.1 mmol dm^{-3} L-cystine in aqueous 2.0 mol dm^{-3} hydrochloric acid, which is typically used in electrosynthesis of the thiol, a very similar set of kinetic parameters is observed.

3.5. The diffusion coefficient of L-cystine from sampled d.c. polarography

For a diffusion limited current in sampled d.c. polarograms at 298 K, Ilkovic derived the expression [16]

$$j_L = 708 z D^{1/2} c_b \left(\frac{dw}{dt}\right)^{2/3}, \tag{19}$$

where j_L is in μA cm^{-2}, D in cm^2 s^{-1}, c_b in mol m^{-3}, $(\frac{dw}{dt})$ is the mass flow rate of mercury in mg s^{-1} (determined by weighing a measured number of mercury drops) and t is the drop time in s. Measurement of j_L allows D to be determined, provided that z and c_b are known. From Eq. (19), the diffusion coefficient of L-cystine in aqueous 0.1 mol dm^{-3}

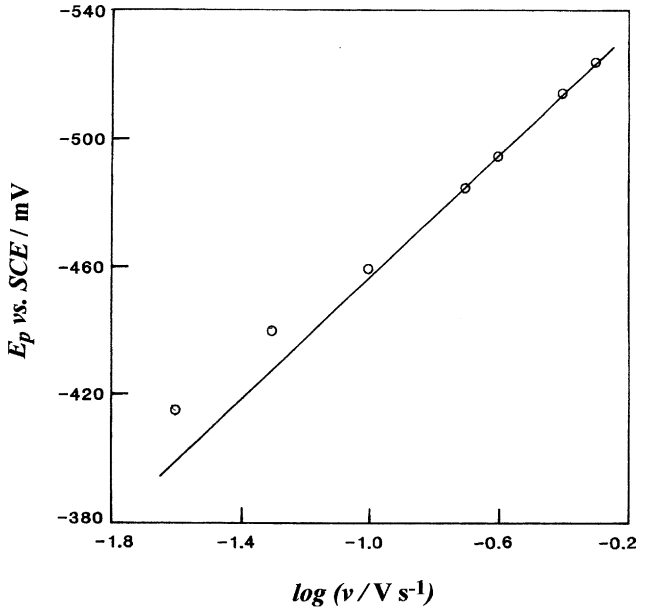

Fig. 7. Dependence of peak potential on the logarithm of the potential sweep rate for linear sweep voltammograms of L-cystine reduction at a HMDE. 0.1 mmol dm^{-3} L-cystine in 0.1 mol dm^{-3} HCl deoxygenated with N_2 at 298 K. The points are the average of five separate measurements.

Table 2
Kinetic parameters from sampled d.c. and linear sweep voltammetry at a mercury drop

Kinetic parameter	Sampled d.c. polarography		Linear sweep voltammetry
	$\log k_f$ vs. E	$-\log[1/j - 1/j_L]$ vs. E	E_p vs. $\log v$
b_c/mV decade^{-1}	-183 ± 4	-183 ± 2	-187 ± 6
α_c	0.32 ± 0.02	0.32 ± 0.01	0.32 ± 0.02

0.1 mmol dm^{-3} L-cystine in aqueous 0.1 mol dm^{-3} HCl at 298 K.

hydrochloric acid is 5.3×10^{-10} m^2 s^{-1} at 298 K. This agrees well with the available literature values of 4.8×10^{-10} m^2 s^{-1} [20] and 5.3×10^{-10} m^2 s^{-1} [21]. In more concentrated, aqueous 2.0 mol dm^{-3} hydrochloric acid solution, the diffusion coefficient is reduced to 4.2×10^{-10} m^2 s^{-1} at 298 K. No literature values are available to compare diffusion coefficient values in the more concentrated acid.

3.6. Effect of adsorption of L-cystine at the mercury surface on the electrode kinetics of the electrosynthesis reaction

The peak for reduction of adsorbed L-cystine in cyclic voltammograms indicates that the disulphide is adsorbed at mercury at potentials just positive of the main reduction wave for dissolved L-cystine. If the adsorption process can be described by the Langmuir adsorption isotherm, it has been shown [22] that

$$\frac{1}{\tau} = \frac{1}{\tau_s} + \frac{1}{\tau_s \beta' c_b}, \tag{20}$$

where τ is the surface excess of adsorbate, τ_s the surface excess corresponding to saturation coverage, β' the adsorption coefficient and c_b the bulk concentration of adsorbent. For L-cystine adsorption at mercury τ can be calculated from the peak in cyclic voltammograms, since by definition

$$\tau = \frac{q_p}{zFA}, \tag{21}$$

where q_p is the charge under the adsorption peak in the voltammogram.

From Eq. (20) a plot of $1/\tau$ against $1/c_b$ is a straight line and τ_s can be calculated from the intercept. Fig. 8 shows at the HMDE a plot of $1/\tau$ against $1/c_b$ is a straight line for adsorption of L-cystine. From the intercept, using a least squares analysis, τ_s is estimated to be $(2.7 \pm 0.8) \times 10^{-7}$ mol m^{-2}. Based upon this saturation coverage, the surface coverage increases from 0.01 to 0.68 as the bulk disulphide concentration is raised from 0.025 to 0.1 mmol dm^{-3}.

Stankovich and Bard [13] constructed a model of L-cystine and, with the disulphide bond orientated on the electrode surface, calculated that a monolayer coverage, corresponded to 2.3×10^{-6} mol m^{-2}. They confirmed this value from the constant peak area in cyclic voltammograms recorded at pH 7.4 at bulk disulphide concentrations of 0.05 mmol dm^{-3} and above. This is a factor of 10 larger than the saturation coverage, τ_s, with adsorption from aqueous 0.1 mol dm^{-3} hydrochloric acid. There may be several reasons why monolayer coverage is achieved at pH 7.4 but is not experienced in acid media. It is possible that the L-cystine molecule must replace protons in the double layer to itself adsorb at the electrode surface at lower pH. The ionised forms of L-cystine at a given solution pH may also help to partially explain the effect. At pH 7.4, the carboxyl groups are deprotonated and there is a resultant attraction to the positively charged amino groups, which may reduce the surface area occupied by the disulphide molecule.

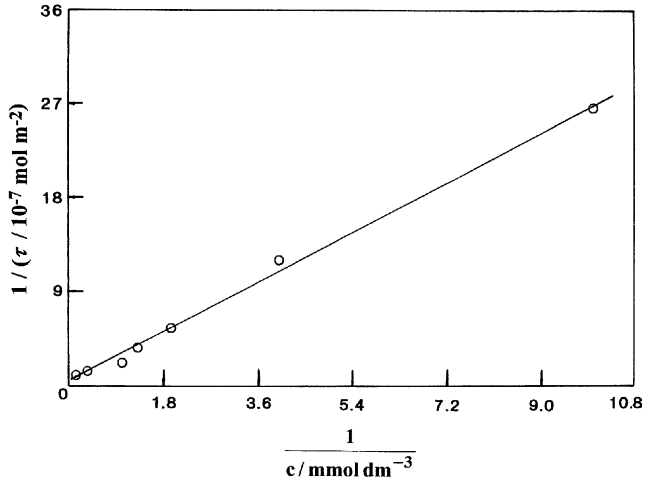

Fig. 8. Reciprocal of surface area coverage vs. reciprocal of bulk electrolyte concentration for L-cystine adsorption from 0.1 mol dm^{-3} HCl at a HMDE. The electrolyte was deoxygenated with N_2 at 298 K.

At the HMDE, for θ between 0.01 and 0.68, values of $-\log[1/j - 1/J_L]$ are plotted against log (L-cystine concentration) at various electrode potentials in Fig. 9. The plot indicates the reaction is first order in the disulphide. Consequently over this range of surface coverage k_f^o and the electrode kinetics are unaltered. At much higher concentrations of the disulphide, however, there is clear evidence of further adsorption of the amino acid on the main electrochemically irreversible wave for reduction of L-cystine to L-cysteine (Fig. 4). At these more negative electrode potentials electrostatic adsorption is expected to be stronger since the disulphide molecule has a double positive charge in acid electrolytes. It seems likely that reduction of dissolved L-cystine occurs through an adsorbed film of the disulphide.

3.7. Effect of pH on the voltammograms

The low solubility of the disulphide at pH > 2 restricts studies to L-cystine concentrations below 0.5 mmol dm^{-3}. The cyclic voltammograms together with sampled d.c. and differential pulse polarograms recorded in the buffer solutions of 2.2–12 show comparable features to those in acid media. Once major difference is that, above pH 2, there are two clear current responses in the sampled d.c. polarograms for reduction of adsorbed and dissolved L-cystine. Indeed, the current plateau for the reduction of the adsorbed material becomes progressively more visible at higher pH as shown in Fig. 10. This may reflect the higher saturation coverage at higher pH.

As predicted by electrode reactions (1) and (3), both reduction waves shift cathodically as the pH is increased. From pH 1 to 13 the move is approximately −59 mV/pH unit, as suggested by the electrode reactions.

3.8. Mechanism of the electrosynthesis of L-cysteine

The mechanism of this reduction has been studied by us at a lead cathode [10]. In this case, the first electron transfer to L-cystine controls the rate of reduction and proton transfer may either precede or occur simultaneously with the first electron transfer, as shown by the sequence:

$$RSSR + H^+ + e^- \overset{RDS}{\rightarrow} RSH + RS^o \quad (22)$$

$$RS^o + H^+ + e^- \rightleftharpoons RSH \quad (23)$$

Both the lower α_c value of 0.32 and the electrochemical reaction order for L-cystine

$$m_{RSSR} = \left[\frac{\partial - \log[1/j - 1/j_L]}{\partial \log c_{b(RSSR)}}\right]_{E,c_b(H^+)} \quad (24)$$

of +1 as shown by the gradient of 1.0 in Fig. 9 are consistent with this mechanism. In order to confirm a comparable mechanism, the electrochemical reaction order for protons was measured, according to

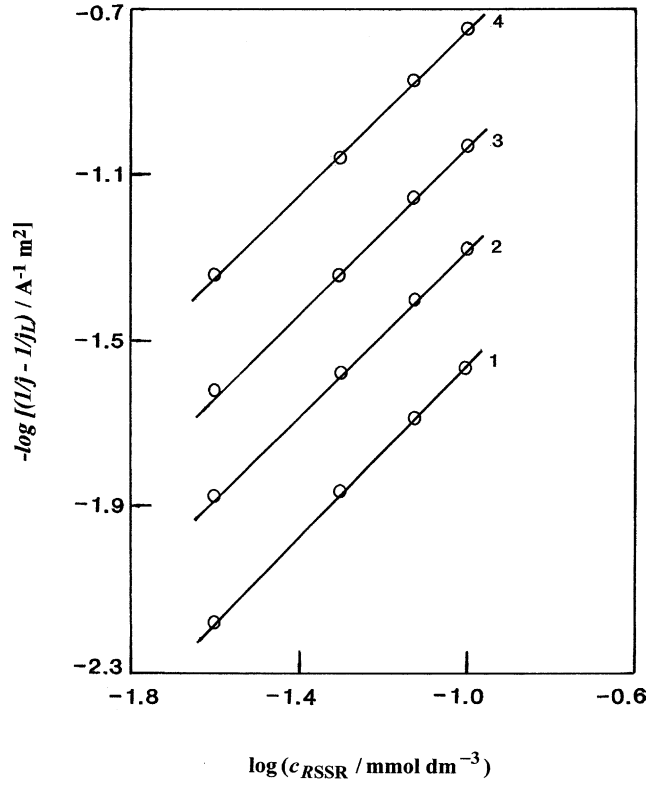

Fig. 9. Plot of $-\log[1/j - 1/j_L]$ against log (RSSR concentration) derived from sampled d.c. polarograms for L-cystine reduction. Potential: (1) −0.145 V; (2) −0.195 V; (3) −0.245 V; (4) −0.295 V vs. SCE. The electrolytes were deoxygenated with N_2 at 298 K.

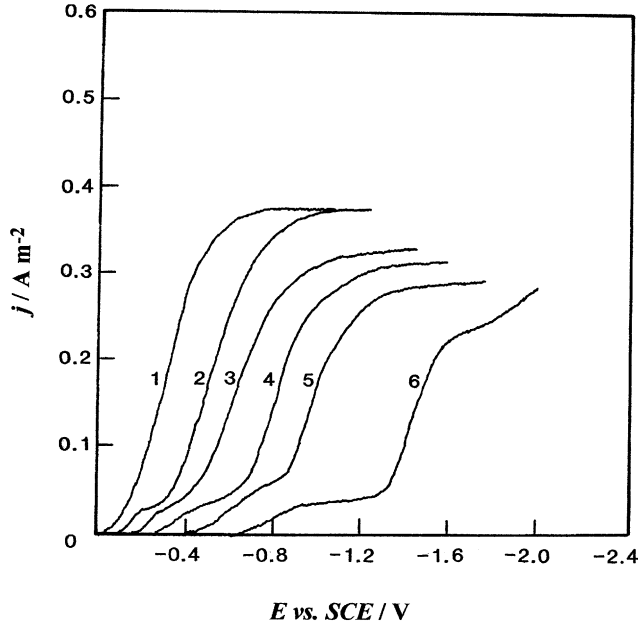

Fig. 10. Variation of sampled d.c. polarograms with electrolyte pH during L-cystine reduction. 0.1 mmol dm^{-3} L-cystine in various electrolytes of constant ionic strength (0.5 mol dm^{-3}) and pH. Electrolytes were deoxygenated with N_2 at 298 K. (1) pH 1.1 (2) pH 2.0 (3) pH 4.0 (4) pH 6.0 (5) pH 9.0 and (6) pH 13.0. 1 drop s^{-1}, $v = 2$ mV s^{-1}.

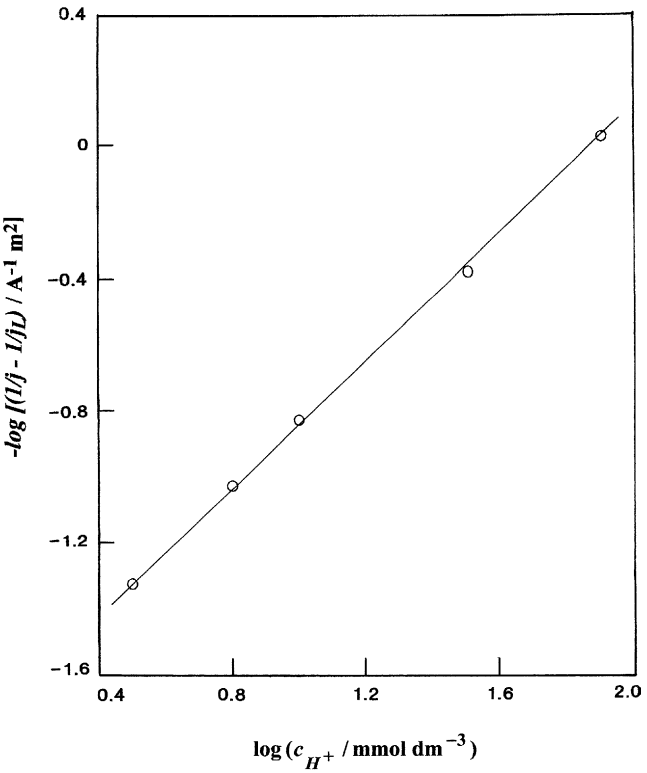

Fig. 11. Plot of $-\log[1/j - 1/j_L]$ against log (H^+ concentration) derived from sampled d.c. polarograms of L-cystine reduction at a potential of −0.295 V vs. SCE. 0.1 mmol dm^{-3} L-cystine in aqueous HCl and KCl solutions of constant pH and ionic strength. The electrolyte was deoxygenated with N_2 at 298 K.

$$m_{H^+} = \left[\frac{\partial - \log[1/j - 1/j_L]}{\partial \log c_{b(H^+)}}\right]_{E,c_{b(RSSR)}} . \quad (25)$$

Fig. 11 shows the plot of $-\log[1/j - j/j_L]$ against $\log c_b(H^+)$ from sampled d.c. polarograms, which were recorded at a constant L-cystine concentration in aqueous background electrolytes of constant pH and constant ionic strength to negate possible salt and double layer effects. From the slope of the straight line the electrochemical reaction order is also +1 for the protons. The mechanism appears to be very similar at high hydrogen overpotential mercury and lead cathodes.

4. Conclusions

1. The reduction of L-cystine to L-cysteine has been studied at mercury drop electrodes in 0.1 mol dm^{-3} HCl, 2 mol dm^{-3} HCl and in buffer solutions of controlled pH in the range pH 1 to pH 13 at 298 K.
2. While the Tafel slope is high at -182 mV $decade^{-1}$ and the cathodic transfer coefficient low at 0.32 (which are the same as the values measured at lead) the rate of the reduction is much faster at mercury than at lead.
3. The high cathodic Tafel slope for reduction of L-cystine probably reflects the effect of adsorption of the disulphide at the cathode potentials where the amino acid is reduced. There is a peak for the reduction of adsorbed L-cystine in the voltammograms at potentials slightly positive of the main wave for L-cystine reduction that obeys the Langmuir isotherm at low coverages ($0.0 < \theta < 0.68$). There is also evidence at higher disulphide concentrations of disulphide adsorption at more negative potentials where the amino acid is reduced. In cyclic voltammograms there is a sharp step in the current, typical of adsorption phenomena, and there are capillary maxima in the sampled d.c. and differential pulse polarograms.
4. The mechanism of reduction is comparable at mercury and lead; the first electron transfer to L-cystine is the rate determining step.
5. The diffusion coefficient of L-cysteine is 5.3×10^{-10} $m^2\ s^{-1}$ in aqueous 0.1 mol dm^{-3} hydrochloric acid and 4.2×10^{-10} $m^2\ s^{-1}$ in aqueous 2.0 mol dm^{-3} hydrochloric acid at 298 K.

Acknowledgement

These studies were supported, in part, by EPSRC funding.

References

[1] T.R. Ralph, M.L. Hitchman, J.P. Millington, F.C. Walsh, J. Electroanal. Chem. 375 (1994) 17.
[2] T.R. Ralph, M.L. Hitchman, J.P. Millington, F.C. Walsh, J. Electroanal. Chem. 375 (1994) 1.
[3] G. Sanchez-Cano, V. Montiel, A. Aldaz, Tetrahedron 47 (4–5) (1991) 877.
[4] A. Aldaz, V. Montiel, J. González-García, V. Garcia-Garcia, in: Proceedings of the 11th International Forum on Electrolysis in the Chemical Industry: Electrochemical Processing Technologies, FL, 2–6 November, 1997.
[5] J. González-Garcia, V. Garcia-Garcia, V. Montiel, A. Aldaz, J. Electrochem. Soc. 148 (2001) D24.
[6] M.L. Hitchman, J.P. Millington, T.R. Ralph, F.C. Walsh, I. Chem. E. Symp. Ser. 127 (1992) 23.
[7] M.L. Hitchman, J.P. Millington, T.R. Ralph, F.C. Walsh, I. Chem. E. Symp. Ser. 112 (1989) 222.
[8] T.R. Ralph, M.L. Hitchman, J.P. Millington, F.C. Walsh, J. Electroanal. Chem. 462 (1999) 97.
[9] T.R. Ralph, M.L. Hitchman, J.P. Millington, F.C. Walsh, Electrochim. Acta. Chem. 51 (2005) 133.
[10] T.R. Ralph, M.L. Hitchman, J.P. Millington, F.C. Walsh, J. Electroanal. Chem. 583 (2005) 260.
[11] D.D. Perrin, B. Dempsey, Buffers for pH and metal ion control, Chapman and Hall Ltd, London, 1974.
[12] A.J. Bard (Ed.), Encyclopedia of Electrochemistry of the Elements, vol. 1, Marcel Dekker, New York, 1973, pp. 167, 250 and 404.
[13] M.T. Stankovich, A.J. Bard, J. Electroanal. Chem. 75 (1977) 487.
[14] M. Fleischman, H.R. Thirsk, Electrochim. Acta 9 (1964) 757.
[15] W.J. Albery, Electrode Kinetics, Clarendon Press, Oxford, 1975 (Chapter 3).

[16] A.J. Bard, L.R. Faulkner, Electrochemical Methods Fundamentals and Applications, second ed., Wiley, New York, 1980, p. 196.
[17] J. Koutecky, Collect. Czech. Chem. Commun. 18 (1953) 597.
[18] J. Weber, J. Koutecky, Collect. Czech. Chem. Commun. 20 (1955) 980.
[19] R.S. Nicholson, I. Shain, Anal. Chem. 36 (1964) 706.
[20] I.M. Issa, A.A. El Samahy, R.M. Issa, Y.M. Temerik, Electrochim. Acta 17 (1972) 1615.
[21] I.M. Kolthoff, C. Barnum, J. Am. Chem. Soc. 63 (1941) 520.
[22] H. Matsuda, Y. Ayabe, Z. Elektrochem. 63 (1959) 1164.